Solid State Communications 152 (2012) 41–44

Contents lists available at SciVerse ScienceDirect

Solid State Communications

journal homepage: www.elsevier.com/locate/ssc

Simulation of the first growth phase of single-walled carbon nanotubes using a model based on a cellular automaton

Alejandro León [a,*], Zdenka Barticevic [b], Mónica Pacheco [b]

[a] Facultad de Ingeniería, Universidad Diego Portales, Santiago, Chile

[b] Departamento de Física, Universidad Técnica F. Santa María, Casilla 110 V, Valparaíso, Chile

ARTICLE INFO

Article history:
Received 28 April 2011
Accepted 10 October 2011
by E.Y. Andrei
Available online 20 October 2011

Keywords:
B. Carbon nanotube
B. Growth phase
D. Cellular automata

ABSTRACT

This paper presents a theoretical study on the first growth phase of single-walled carbon nanotubes. The model adopted is based on a cellular automaton containing as the elementary entities the metal particles and the carbon atoms. It uses an interaction based on phenomenological potentials to define the update function of the automaton. The purpose of this study is to establish the saturation condition of the metal particle with the carbon atoms when the formation of clusters of carbon begins. The results show that the first phase of formation of the carbon clusters can start with the particle partially saturated with carbon atoms.

1. Introduction

Carbon nanotubes (CNTs) are quasi-unidimensional systems having electronic, mechanical, and chemical properties that are useful to study in order to develop potential technological applications in many areas [1,2]. Currently, there are large-scale methods to purify and synthesize CNTs [3–8], but still there is not a method to satisfy the demand of the same topology and defect-free nanotubes. The accepted general criterion is that a growth method using catalytic particles would be the most appropriate to synthesize single-walled CNTs [9]. Thus, a great number of theoretical studies have been reported attempting to understand the growth mechanisms of CNTs from metal particles. Models based on classical molecular dynamics (MD) and using phenomenological potentials have analyzed the growth dynamics in different conditions, including those of the supporting substrate for the particle [10–16]. The results provided by those studies have allowed substantial progress in the knowledge of the growth dynamics of nanotubes. Ding et al. [11–14] have shown that the metal particle goes through a phase in which the carbon atoms diffuse, saturating the particle before the nucleation process starts. Another tool used by some groups of researchers is the Car–Parrinello density functional theory [17,18], which sheds light on the first nucleation stages but it is limited by high computational costs. In one of those studies, Gavillet and his collaborators suggested that the segregation of linear carbon chains on the surface of a cobalt particle in the liquid phase would represent the first stages in the nucleation of CNTs. The results of some recently published studies using the density functional based tight binding molecular dynamics (DFTB/MD) approach [19–21], suggest that it is not necessary for the catalytic particle to be saturated with carbon in order to start the nucleation process, a finding that contradicts the results obtained by Ding et al. using classical molecular dynamics.

This paper presents a theoretical study of the thermal diffusion of carbon atoms in iron nanoparticles. A model based on a cellular automaton (CA) is used under different temperature conditions, different sizes of the catalytic nanoparticle, and with different affinity with the substrate supporting the particle. We have considered different conditions of saturation of the particle during the first part of the formation of carbon clusters.

2. Model used for simulation

A variety of models based on CA have been demonstrated to be very efficient for studying the dynamics of the growth of biological and physical structures [22] since they allow the study of highly complex systems with low computational costs. The cells of the automaton are formed by the Fe atoms of the metal particle and the carbon atoms. The state of each cell is a vector containing information about the position of the atom, its energy, its temperature, and the field generated by the neighboring cells (atoms). The schema for the CA is shown in Fig. 1. Notice that the configuration of the neighboring cells varies in every updating step due to the changes in the position of the atoms. That is why the CA used in this model will be called a dynamic cellular automaton (DCA).

The update function depends on the state of each single cell, on the state of the neighboring cells, and on the interactions between the atoms, which is achieved from the phenomenological

* Corresponding author.
E-mail address: alejandro.leon@udp.cl (A. León).

0038-1098/$ – see front matter © 2011 Elsevier Ltd. All rights reserved.
doi:10.1016/j.ssc.2011.10.011

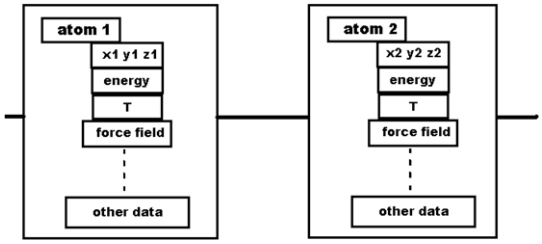

Fig. 1. Schema of the cells forming the DCA.

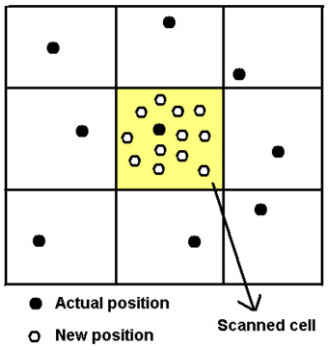

Fig. 2. Schema of the update of each cell.

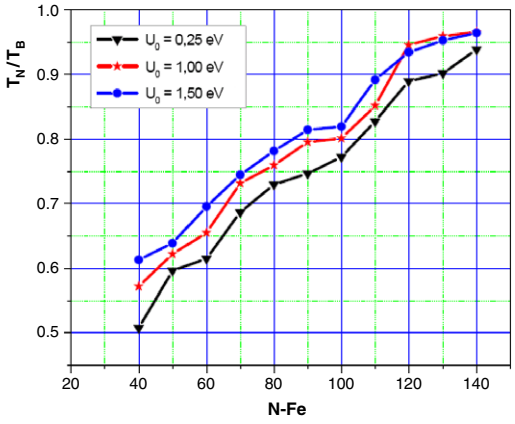

Fig. 3. Transition phase of the nanoparticle as a function of the number of atoms.

potentials. The interaction between Fe atoms is modeled by means of the multi-body potential with parameters obtained from the work of Shibuta and Maruyama [16]. The interaction of the metal atoms with the substrate is modeled using a one-dimensional Lennard-Jones potential, which considers the interaction of an Fe atom with all the atoms on the surface of the substrate. This potential has the following form:

$$U(z) = U_0 \left(\frac{1}{5} \left(\frac{z}{\sigma} \right)^{-10} - \left(\frac{z}{\sigma} \right)^{-4} \right). \tag{1}$$

The energy parameter U_0 quantifies the affinity of the nanoparticle with the substrate and the distance parameter σ is considered as the van der Waals radius of the silicon atoms, $\sigma = 3.23$ Å. This model considers a flat, ideal, and inert substrate. The valor of this parameter correspond to the silica. The interaction of the Fe atoms with the carbon atoms is modeled using the Johnson potential [23] given by the equation

$$E(r) = -\varepsilon \left(2 \left(\frac{r^* - \gamma}{\gamma - 1} \right)^3 + 3 \left(\frac{r^* - \gamma}{\gamma - 1} \right)^2 \right). \tag{2}$$

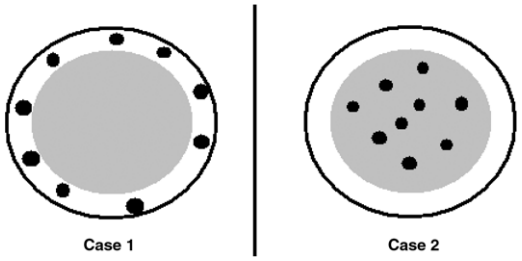

Fig. 4. Cases 1 and 2, showing the regions where the carbon atoms are injected into the nanoparticle.

The parameters $r^* = r/r_0$ and $\gamma = r_C/r_0$ are obtained from experimental data [24]. Finally, two types of interaction are considered for the carbon atoms. First, if the atoms are inside the Fe particle they are considered as being dissolved, and the C–C interaction is modeled with a 6–12 Lennard-Jones potential. The interactions between carbon atoms on the surface and outside the particle are modeled by means of the Brenner potential [25].

The global update of the DCA is achieved in the following manner.

(1) The automaton is scanned, and in each cell 100 new atomic positions are randomly chosen around the corresponding original atomic position. This is represented in Fig. 2.

(2) For each one of the 100 new positions, the energy of the atom in the cell is determined by using phenomenological potentials for the interaction with the neighbor cells.

(3) Using a genetic algorithm [26], steps (1) and (2) are repeated, with some defined criteria, in order to minimize the local energy in the cell. The lowest energy position is accepted.

(4) The new positions for each atom are accepted with a probability $P = \exp(-\beta \Delta E)$ if $\Delta E \geq 0$, and with $P = 1$ when $\Delta E < 0$. In these expressions, $\beta = \frac{1}{kT}$, and ΔE is the energy difference between the current state and the past state of the cell.

3. Results and discussion

3.1. Fusion temperature of the nanoparticle

The first study realized was the calculation of the melting temperature of the catalytic particle as a function of the number of atoms in it. For this, we use the so-called Lindemann index, defined as

$$\delta = \frac{2}{N(N-1)} \sum_{i<j} \frac{\sqrt{\langle r_{ij}^2 \rangle - \langle r_{ij} \rangle^2}}{\langle r_{ij} \rangle}, \tag{3}$$

where r_{ij} is the distance between the atoms i and j, and N is the number of atoms in the nanoparticle.

Fig. 3 shows the melting temperature T_N of the nanoparticle in units of the corresponding temperature T_B of iron under atmospheric pressure. Three cases of affinity with the substrate were studied, determining the Lindemann index and hence the melting point. Fig. 3 shows that the melting temperature increases when the interaction with the substrate increases. Such a result would be qualitatively consistent with other studies on the phase transition of nanoparticles [27,28], and with the behavior that predicts the Gibbs–Thomson equation.

3.2. Saturation in the thermal diffusion

In order to study the saturation condition in the thermal diffusion process, we have used the following methodology. First, the diffusion process is simulated by injecting carbon atoms inside the particle at a constant time rate and in two different regions.

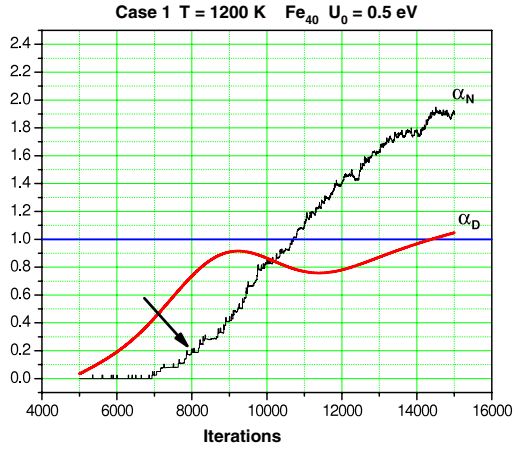

Fig. 5. Study for a particle with 40 atoms in case 1 and $T = 1200$ K.

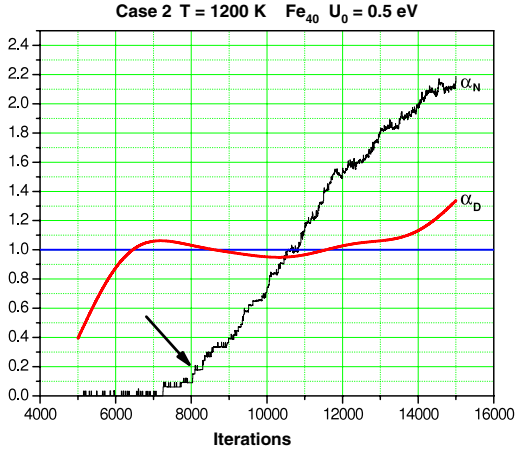

Fig. 6. Study for a particle with 40 atoms in case 2 and $T = 1200$ K.

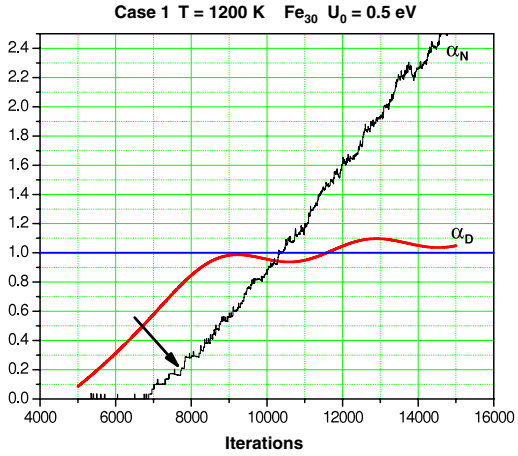

Fig. 7. Study for a particle with 30 atoms in case 1 and $T = 1200$ K.

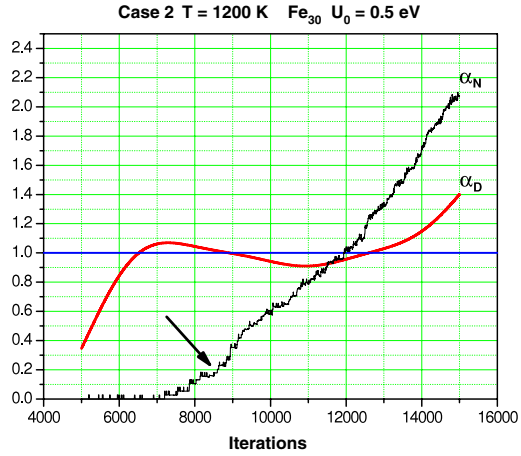

Fig. 8. Study for a particle with 30 atoms in case 2 and $T = 1200$ K.

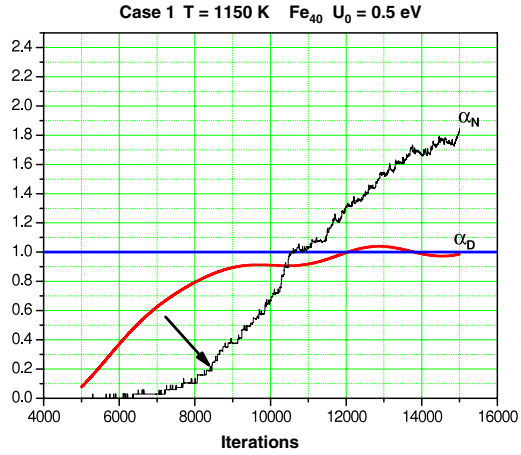

Fig. 9. Study for a particle with 40 atoms in case 1 and $T = 1150$ K.

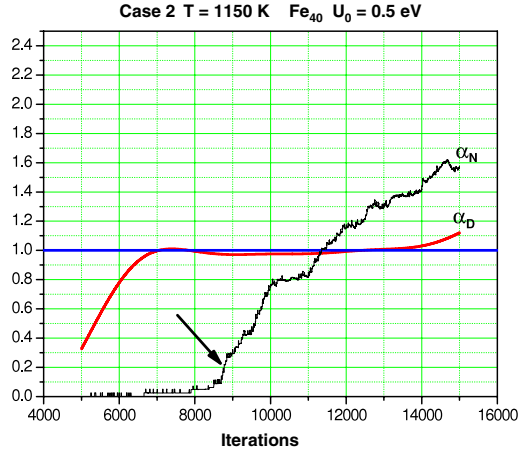

Fig. 10. Study for a particle with 40 atoms in case 2 and $T = 1150$ K.

Although this process does not simulate a real situation, it allows us to study different saturation conditions. We proceed to divide the volume of the particle into an external region with $0.9R \leq r \leq R$ (Case 1) and another internal region with $r < 0.9R$ (Case 2), where R represents the particle means radius, as shown in Fig. 4.

The index α_D is defined as $\alpha_D = \frac{C_1}{C_0}$, where C_1 is the number of carbon atoms diffused into the particle and C_0 is the number of carbon atoms, separated by the equilibrium distance given by Lennard-Jones potential, in a volume equal to the volume of the nanoparticle. The α_N index is defined as $\alpha_N = \frac{N_1}{N_0}$, where N_1 is the number of carbon atoms that have formed covalent bonds on the surface of the particle and beyond. N_0 represents the number of carbon atoms arranged in a structure of graphene, in the half of the surface of a sphere with radius equal to the radius of the nanoparticle. Let us define the beginning of the formation of covalent bonds, when $\alpha_N = 0.2N_0$. Figs. 5 and 6 show the results obtained for a particle with 40 Fe atoms, with an interaction energy with the substrate of $U_0 = 0.5$ eV and a temperature of 1200 K.

The results shown in Fig. 5 (Case 1) indicate that the formation of covalent bonds begins when the particle is saturated in 70% of carbon atoms. In contrast, Fig. 6 (Case 2) shows that the formation of carbon clusters begins with the particle fully saturated.

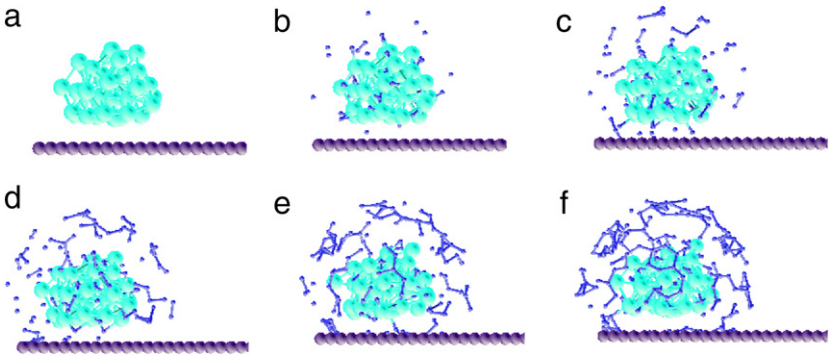

Fig. 11. Schema for the thermal diffusion of the study shown in Fig. 9.

This behavior is repeated when we study a particle with 30 Fe atoms (Figs. 7 and 8), with an interaction energy with the substrate of $U_0 = 0.5$ eV and a temperature of 1200 K. Fig. 7 (Case 1) shows that the process of carbon clusters formation begins when the particle is 75% saturated with carbon atoms. Fig. 8 (Case 2) shows that the process begins when the particle is 100% saturated with carbon atoms.

In the case of a particle with 40 atoms of Fe and a temperature of 1150 K the behavior is similar to previous studies. These results are shown in Figs. 9 and 10.

Fig. 11 shows a schema of the thermal diffusion at the following times (in DCA update units): (a) $t_1 = 5000$, (b) $t_1 = 7000$, (c) $t_1 = 9000$, (d) $t_1 = 11{,}000$, (e) $t_1 = 13{,}000$, (f) $t_1 = 15{,}000$, respectively. At the time equivalent to 5000 iterations, the process of injection of carbon atoms begins. These schemas correspond to Case 1 in Fig. 9. The big spheres represent the Fe atoms, the medium-size spheres represent the atoms of the substrate, and the small spheres represent the carbon atoms.

A similar study was carried out by comparing Cases 1 and 2 for different values of the U_0 parameter, which represents the affinity with the substrate, for different temperature values and different values of the number of Fe atoms of the catalyst particle. The results show a qualitative behavior similar to that shown in Figs. 5–10.

4. Conclusions

A study of the thermal diffusion of carbon atoms in iron nanoparticles has been carried out, using a model based on a dynamic cellular automaton. The results show that the first phase of formation of the carbon clusters can start with the particle partially saturated with carbon atoms. Such a result would be consistent with some other studies of quantum molecular dynamics that predict a similar behavior. One of the main results of this study is that, by analyzing the carbon structures that are formed with both methods—initially saturated and non-saturated particles, it is found that the number of defects is much higher in those structures formed using non-saturated particles. We have also concluded that the catalytic particle experiments several changes in size during the nucleation process, a finding consistent with the changes in phases of the Fe–C compounds.

Acknowledgments

The authors acknowledge the financial support of FONDECYT program grants 1100672, 11100045 and USM 110971 internal grant.

References

[1] M.S. Dresselhaus, G. Dresselhaus, P. Avouris, Carbon Nanotube: Synthesis, Structure, Properties, and Applications, Springer, New York, 2001.
[2] R.A. Baughman, A.A. Zakhidov, W.A. de Heer, Science 297 (2002) 787–792.
[3] A. Thess, R. Lee, P. Nikolaev, H. Dai, P. Petit, J. Robert, C. Xu, Y.H. Lee, S.G. Kim, A.G. Rinzler, D.T. Colbert, G.E. Scuseria, D. Tománek, J.E. Fischer, R.E. Smalley, Science 273 (1996) 483.
[4] C. Journet, W.K. Maser, P. Bernier, A. Loiseau, M.K. de la Chapelle, S. Lefrant, P. Deniard, R. Lee, E. Fisher, Nature 388 (1997) 756.
[5] H. Dai, A.G. Rinzler, P. Nikolaev, A. Thess, D.T. Colbert, R.E. Smalley, Chem. Phys. Lett. 260 (1996) 471.
[6] P. Nikolaev, M.J. Bronikowski, R.K. Bradley, F. Rohmund, D.T. Colbert, K.A. Smith, R.E. Smally, Chem. Phys. Lett. 313 (1999) 91.
[7] Y. Murakami, S. Chiashi, Y. Miyauchi, M. Hu, M. Ogura, T. Okubo, S. Maruyama, Chem. Phys. Lett. 385 (2004) 298.
[8] K. Hata, D.N. Futaba, K. Mizuno, T. Namai, M. Yumura, S. Iijima, Science 306 (2004) 1362.
[9] S. Irle, Y. Ohta, Y. Okamoto, A.J. Page, Y. Wang, K. Morokuma, Nano Res. 2 (2009) 755–767.
[10] Y. Shibuta, S. Maruyama, Physica B 323 (2002) 187–189.
[11] Y. Shibuta, S. Maruyama, Chem. Phys. Lett 382 (2003) 381–386.
[12] F. Ding, K. Bolton, A. Rosen, J. Phys. Chem. B 108 (2004) 17369–17377.
[13] F. Ding, K. Bolton, A. Rosen, J. Phys. Chem. B 121 (2004) 2775–2779.
[14] F. Ding, K. Bolton, A. Rosen, J. Vac. Sci. Technol. A 22 (2004) 1471–1476.
[15] F. Ding, K. Bolton, A. Rosen, Comput. Mater. Sci. 35 (2006) 243–246.
[16] Y. Shibuta, S. Maruyama, Comput. Mater. Sci. 39 (2007) 842–848.
[17] J. Gavillet, A. Loiseau, C. Journet, F. Willaime, F. Ducastelle, J. Charlier, Phys. Rev. Lett. 87 (2001) 275504.
[18] J.Y. Raty, F. Gygi, G. Galli, Phys. Rev. Lett. 95 (2005) 096103.
[19] Y. Ohta, S. Irle, Y. Okamoto, K. Morokuma, ACS Nano 2 (2008) 1437–1444.
[20] Y. Ohta, S. Irle, Y. Okamoto, K. Morokuma, J. Phys. Chem. C 113 (2009) 159–169.
[21] Y. Ohta, S. Irle, Y. Okamoto, K. Morokuma, Carbon 47 (2009) 1270–1275.
[22] D. Griffeath, C. Moore (Eds.), New Constructions in Cellular Automata, University Press, Oxford, 2003.
[23] R.A. Johnson, Phys. Rev. A 134 (1964) 1329.
[24] A.V. Evteev, A.T. Kosilov, E.V. Levtchenko, in: Proceeding of the 22nd Riso International Symposium on Material Science, 2001.
[25] D.W. Brenner, Phys. Rev. B 42 (1990) 9458.
[26] D. Asholock, Evolutionary Computation for Modeling and Optimization, Springer, 2006.
[27] Y. Shibuta, T. Suzuki, Chem. Phys. Lett. 445 (2007) 265.
[28] Y. Shibuta, T. Suzuki, J. Chem. Phys. 129 (2008) 144102.